

# Low Noise $\text{In}_{0.32}(\text{AlGa})_{0.68}\text{As}/\text{In}_{0.43}\text{Ga}_{0.57}\text{As}$ Metamorphic HEMT on GaAs Substrate with 850 mW/mm Output Power Density

C. S. Whelan, W. E. Hoke, R. A. McTaggart, S. M. Lardizabal, P. S. Lyman, P. F. Marsh, and T. E. Kazior

**Abstract**—A double-pulse-doped  $\text{InAlGaAs}/\text{In}_{0.43}\text{Ga}_{0.57}\text{As}$  metamorphic high electron mobility transistor (MHEMT) on a GaAs substrate is demonstrated with state-of-the-art noise and power performance. This 0.15- $\mu\text{m}$  T-gate MHEMT exhibits high on- and off-state breakdown ( $V_{ds} > 6$  V and  $V_{dp} > 13$  V, respectively) which allows biasing at  $V_{ds} > 5$  V. The 0.6-mm device shows  $>27$  dBm output power (850 mW/mm) at 35 GHz—the highest reported power density of any MHEMT. Additionally, a smaller gate periphery  $2 \times 50 \mu\text{m}$  (0.1 mm) 43% MHEMT exhibits a  $F_{\text{min}} = 1.18$  dB and 10.7 dB associated gain at 25 GHz, and also is the first noise measurement of a  $\sim 40\%$  In MHEMT. A double recess process with selective etch chemistries provides for high yields.

**Index Terms**—GaAs, HEMT, InP, metamorphic, MHEMT, noise, power.

## I. INTRODUCTION

WHILE InP HEMT's (53–60% In content channels) have shown high gain and low noise at millimeter-wave frequencies, their low on-state breakdown voltage has limited their use in power applications. Conversely, GaAs PHEMT's (15–20% In) show excellent power and gain at microwave frequencies, but their millimeter-wave performance is limited by a relatively low  $F_t$  of  $\sim 70$  GHz. These limitations can be overcome by using metamorphic HEMT technology—growth of a high In content channel on a GaAs substrate. Metamorphic high electron mobility transistors (MHEMT's) [1]–[5] provide the ability to tailor the lattice constant to any indium content channel desired, and therefore allow the device designer an additional degree of freedom to optimize the transistor for high frequency gain, power, and low noise. Previously, 30–40% In MHEMT's have demonstrated impressive dc and gain performance, but power performance has been limited ( $<250$  mW/mm) by low on-state breakdown which restricts drain bias voltages to less than 3.5 V [6], [7]. Recently, 6 V drain biasing has been achieved on 32% In MHEMT's, resulting in output powers of 825 mW/mm at X-band [8] and 650 mW/mm at 35 GHz [9]. We have built on these early results and applied them to our 43% In MHEMT, where we now report 6 V drain biasing for the first time on a  $\sim 40\%$  In MHEMT. This biasing results in the highest reported power density of any MHEMT, while the 43% In channel produces low noise.

Manuscript received August 24, 1999; revised October 1, 1999. The review of this letter was arranged by Editor D. Ueda.

The authors are with the Raytheon RF Components, Advanced Device Center, Andover, MA 01810 USA.

Publisher Item Identifier S 0741-3106(00)00432-8.

## II. MATERIAL AND PROCESSING

The double pulse doped  $\text{In}_{0.32}(\text{AlGa})_{0.68}\text{As}/15$  nm  $\text{In}_{0.43}\text{Ga}_{0.57}\text{As}/\text{In}_{0.32}(\text{AlGa})_{0.68}\text{As}$  MHEMT was grown on a  $\sim 1 \mu\text{m}$  graded buffer layer [10], yielding a 300K mobility of  $8800 \text{ cm}^2/\text{V}\cdot\text{s}$  and a 77K mobility of  $27000 \text{ cm}^2/\text{V}\cdot\text{s}$ . The Al/Ga ratio of the  $\text{AlGaInAs}$  barrier layer was adjusted to give a bandgap of 1.7–1.8 eV. The conduction band discontinuity of this structure is nominally 0.6–0.7 eV (calculated from measured data), allowing sheet densities at least as high as  $4.0 \times 10^{12} \text{ cm}^{-2}$ . To optimize the trade-off between  $I_{\text{max}}$  and breakdown voltage, the Si pulse densities were reduced to attain a sheet density of  $3.0 \times 10^{12} \text{ cm}^{-2}$  for maximum output power. Noise performance was also a consideration in choosing the proper sheet density. A cross section of the  $\text{In}_{0.43}\text{Ga}_{0.57}\text{As}/\text{In}_{0.32}(\text{AlGa})_{0.68}\text{As}$  MHEMT structure is shown in Fig. 1.

Device fabrication begins with mesa isolation down to the graded buffer layer by wet chemical etching using a  $\text{H}_2\text{SO}_4:\text{H}_2\text{O}_2:\text{H}_2\text{O}$  mixture. Ni–Au–Ge–Au ohmic metal is evaporated and hot-plate annealed, yielding a transmission line model (TLM) extracted contact resistance of  $0.08 \Omega/\text{mm}$ . The device employs a double recess structure, where the channel and gate recesses are formed using succinic/peroxide selective wet etches and stop layers, dramatically improving the manufacturability and repeatability of the most critical process steps. The resulting standard deviation across a 3-in wafer is less than 5% for  $I_{\text{dss}}$ ,  $I_{\text{max}}$ ,  $V_{po}$  ( $I_{\text{ds}} = 1 \text{ mA/mm}$ ) and  $G_m$ . An 0.15- $\mu\text{m}$  Ti/Pt/Au T-gate is deposited, followed by  $\text{SiN}_x$  passivation. Finally, individual source vias are reactive ion etched (RIE) through the thinned 2 mil substrate to lower the source inductance and to provide thermal dissipation.

## III. DEVICE PERFORMANCE

Completed MHEMT devices underwent dc, small signal RF, power, and noise testing. A typical dc  $I$ – $V$  curve for an 0.1-mm device is shown in Fig. 2. An  $I_{\text{max}}$  of 650 mA/mm was achieved at  $V_{gs} = +1$  V, with low output conductance and little kink effect. The output conductance was  $\sim 25 \text{ mS/mm}$  at  $I_{\text{dss}}$  and  $V_{ds} = 2$  V. This is one of the very few published MHEMT family of current-voltage ( $I$ – $V$ ) curves that has been swept to  $V_{ds} = 2.5$  V at  $I_{\text{max}}$ , due to their low on-state breakdowns. Fig. 3 demonstrates over 6 V drain bias at 225 mA/mm without avalanche breakdown. The gate current  $|I_{gs}|$  at  $V_{ds} = 6$  V,  $I_{ds} = 225 \text{ mA/mm}$  bias is still  $<1 \text{ mA/mm}$ , whereas most InP HEMT's with similar gate lengths and sheet densities show

240-7

500Å InGaAs $5 \times 10^{18} \text{ cm}^{-3}$ In = 32%
InAlGaAs Undoped In = 32%
Si Pulse Doping
150Å InGaAs Channel In = 43%
Si Pulse Doping
InAlGaAs Undoped In = 32%
1 $\mu\text{m}$ Buffer Layer
GaAs Substrate

Fig. 1. Cross section of the  $\text{In}_{0.43}\text{Ga}_{0.57}\text{As}/\text{In}_{0.32}(\text{AlGa})_{0.68}\text{As}$  MHEMT structure on a GaAs substrate.

on-state breakdowns of  $\sim V_{ds} = 3 \text{ V}$  ( $|I_{gs}| = 1 \text{ mA/mm}$ ) [11]. We attribute the high on-state breakdown voltage and reduced kink effect to several reasons:

- 1) an additionally inserted valence band discontinuity blocking holes from reaching the  $\text{SiN}_x$ /semiconductor interface;
- 2) the double selective double recess etch process providing excellent uniformity which minimizes spikes in electric field along the gate recess; and
- 3) excellent material quality minimizing defects [12].

These high on-state breakdown results allow operation at high drain biasing (up to  $V_{ds} = 6 \text{ V}$ ) for high-power applications. An off-state gate-drain breakdown voltage of over  $-13.5 \text{ V}$  at  $I_g = 1 \text{ mA/mm}$  is achieved even with an  $I_{max}$  of  $650 \text{ mA/mm}$ . The forward Schottky drain-gate diode turn-on voltage is  $0.85 \text{ V}$ . The quaternary Schottky's  $1.7\text{--}1.8 \text{ eV}$  bandgap is also significantly larger than the conventional  $1.45\text{--}1.6 \text{ eV}$  Schottky layers used in lattice-matched (to InP) devices. The corresponding improvement in barrier height and the relatively low sheet density (for the depth of the well) account for much of this increase in off-state breakdown voltage. A broad extrinsic transconductance peak of  $700 \text{ mS/mm}$  is measured at  $V_{ds} = 1 \text{ V}$ ,  $V_{gs} = 0.1 \text{ V}$ , and remained over  $600 \text{ mS/mm}$  for a  $V_{gs}$  range of  $0.5 \text{ V}$ . Pinchoff voltage is  $V_{gs} = -0.7 \text{ V}$  at  $I_{ds} = 1 \text{ mA/mm}$ .

Small signal S-parameters were measured from 0 to  $45 \text{ GHz}$  on an  $0.1\text{-mm}$  device biased at  $V_{ds} = 1 \text{ V}$  over the full range of gate biases.  $E_s$  (extrapolated from  $H_{21}$  using  $-6 \text{ dB/octave}$ ) reaches a broad maximum of  $128 \text{ GHz}$  at the  $G_m$  peak ( $V_{gs} = -0.1 \text{ V}$ ,  $I_{ds} = 270 \text{ mA/mm}$ ).

The noise performance of  $2 \times 50 \mu\text{m}$  ( $0.1 \text{ mm}$ ) MHEMT devices was measured at  $V_{ds} = 1 \text{ V}$ , over a range of drain current, from 1 to  $25 \text{ GHz}$ . Fig. 4 plots  $F_{min}$  and  $G_{assoc}$  at  $25 \text{ GHz}$  for a MHEMT and a geometrically identical, low-noise 20% InPHEMT. (Both devices showed the lowest noise at  $V_{ds} = 1 \text{ V}$ .) The MHEMT device reaches a broad minimum at  $F_{min} = 1.18 \text{ dB}$  and  $G_{assoc} = 10.7 \text{ dB}$  while the PHEMT only shows  $F_{min} = 1.60 \text{ dB}$  and  $G_{assoc} = 7.6 \text{ dB}$ . The MHEMT shows a clear advantage in noise and gain, with  $0.42 \text{ dB}$  lower  $F_{min}$  and  $3.1 \text{ dB}$  higher gain at  $25 \text{ GHz}$ . Unique to this MHEMT is the low noise over a wide range of currents, making it an ideal candidate for low current satellite applications or high gain appli-

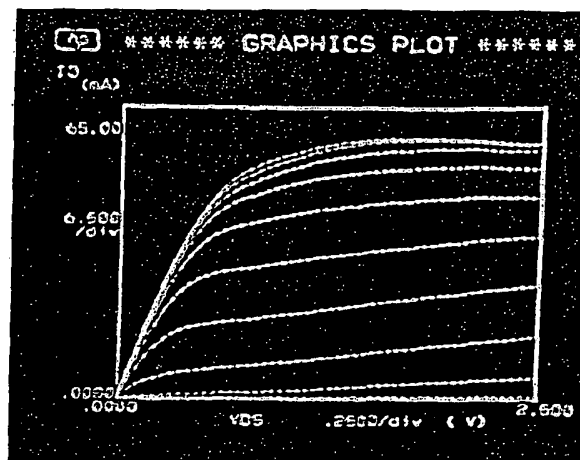


Fig. 2. A 43% In MHEMT DC  $I$ - $V$  curves, with steps of  $V_{gs} = 0.2 \text{ V}$ , show low output conductance and little kink effect. The top  $I$ - $V$  curve shows current swept to  $V_{ds} = 2.5 \text{ V}$  at  $I_{max} = 650 \text{ mA/mm}$  without breakdown.

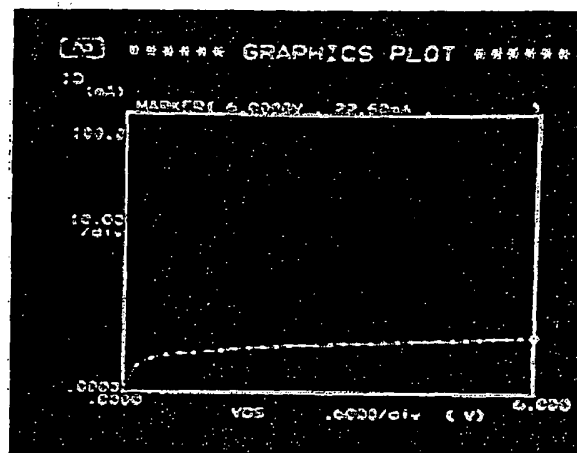


Fig. 3. MHEMT  $I$ - $V$  curve swept to  $V_{ds} = 6 \text{ V}$  at  $I_{ds} = 225 \text{ mA/mm}$  for an  $0.1\text{-mm}$  device without breakdown.

cations with higher currents. This is the first noise performance data for a  $\sim 40\%$  In MHEMT reported.

The power bench consisted of a HP 8350B sweep oscillator and a traveling wave tube amplifier coupled to a HP 438A power meter and power sensor. Tuning was performed manually. The high on- and off-state breakdown voltages of our 43% indium MHEMT allow  $V_{ds} = 5$  and  $6 \text{ V}$  quiescent biasing of the  $12 \times 50 \mu\text{m}$  ( $0.6 \text{ mm}$ ) devices for  $35\text{-GHz}$  power testing. The gate was biased for a drain current of  $150 \text{ mA/mm}$  or about 20% of  $I_{max}$ . These  $0.6\text{-mm}$  devices showed an  $I_{max} = 400 \text{ mA/mm}$ , a  $V_{knee} = 1.03 \text{ V}$  and a drain-gate  $V_{BRK}$  ( $1 \text{ mA/mm}$ )  $= -13 \text{ V}$ . Tuning for a compromise between gain and power, the MHEMT produced  $26.7 \text{ dBm}$  of output power,  $5.3 \text{ dB}$  of associated gain and  $40.4\%$  power added efficiency (PAE) at  $V_{ds} = 6 \text{ V}$ , at  $1 \text{ dB}$  gain compression. Maximum  $P_{out}$  at  $6 \text{ V}$  drain biasing is  $27.1 \text{ dBm}$  under  $2 \text{ dB}$  of compression, normalizing to  $850 \text{ mW/mm}$ . The output power,  $G_{assoc}$  and PAE is plotted versus input power in Fig. 5. At  $5 \text{ V}$  biasing, the MHEMT produced  $830 \text{ mW/mm}$  of output power which far exceeds the  $700 \text{ mW/mm}$  of our best

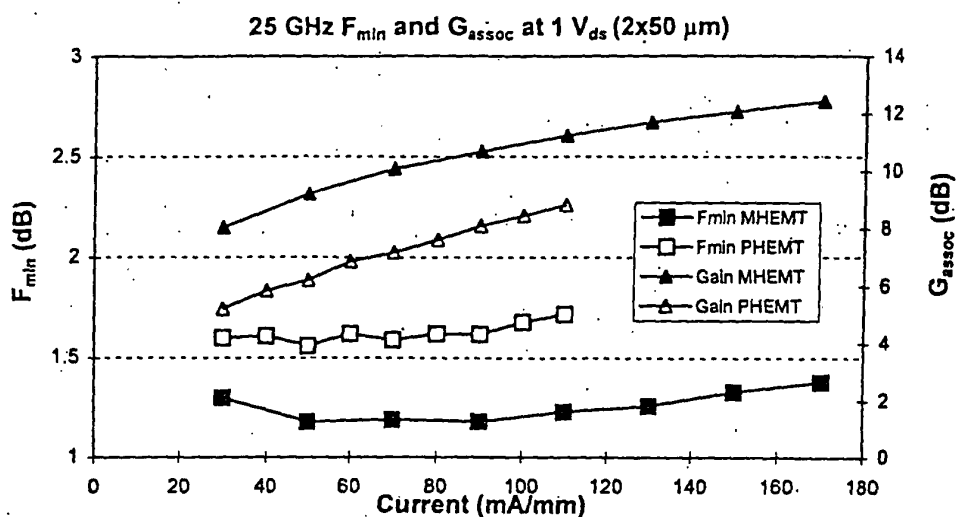


Fig. 4. Comparisons at 25 GHz of an 0.1-mm MHEMT and an 0.1-mm GaAs PHEMT device with 0.15- $\mu\text{m}$  gate lengths biased at  $V_{ds} = 1$  V show that the MHEMT has 0.4 dB lower  $F_{\min}$  and >3 dB more  $G_{\text{assoc}}$ .

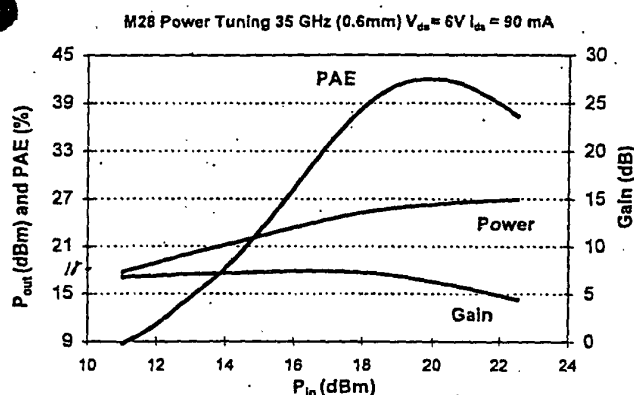


Fig. 5. The 0.6-mm MHEMT device, biased at  $V_{ds} = 6$  V with 0.15- $\mu\text{m}$  gate length, shows 26.7 dBm of power, 5.3 dB of associated gain, and 40.4% power added efficiency at 35 GHz and 1 dB compression.

GaAs PHEMT's at 35 GHz. Backing the output power of the MHEMT off to 700 mW/mm results in >2 dB more associated gain than the GaAs PHEMT at 700 mW/mm. To the best of our knowledge this is the maximum power density and drain biasing of any MHEMT reported (and of most InP HEMT's), and demonstrates MHEMT's ability to deliver excellent power and gain at millimeter-wave frequencies. An increase in doping density to  $3.4 \times 10^{12} \text{ cm}^{-2}$  (accomplished by increasing the pulse doping density) resulted in 920 mW/mm at 6 V drain biasing at a frequency of 35 GHz.

#### IV. SUMMARY

We report on the first high power density, low-noise metamorphic  $\text{In}_{0.32}\text{AlGa}_{0.68}\text{As}/\text{In}_{0.43}\text{Ga}_{0.57}\text{As}$  HEMT grown on a GaAs substrate. The device exhibits comparable breakdown to a GaAs PHEMT, but with significantly lower noise, along and state-of-the-art RF performance. High on- and off-state break-

down allow 6 V drain biasing, resulting in 850 mW/mm of output at 35 GHz for  $3.0 \times 10^{12} \text{ cm}^{-2}$  doping and 920 mW/mm for  $3.4 \times 10^{12} \text{ cm}^{-2}$  doping. This 43% In MHEMT shows a unique combination of high output power and low noise, and could be potentially used in transmit-receive circuits fabricated on the same wafer.

#### ACKNOWLEDGMENT

The authors would like to acknowledge the support of L. Aucoin, Chief Research Scientist of Raytheon RF Components, and thank B. Ingersoll for S-parameter measurements.

#### REFERENCES

- [1] M. Chertouk, H. Heiss, D. Xu, S. Kraus, W. Klein, G. Bohm, G. Trankle, and G. Weimann, "Metamorphic  $\text{InAlAs}/\text{InGaAs}$  HEMT's on GaAs substrates with a novel composite channel design," *IEEE Electron Device Lett.*, vol. 17, pp. 273-275, 1996.
- [2] D. Gill, B. Kane, S. Svensson, D. Tu, P. Uppal, and N. Byer, "High-performance, 0.1  $\mu\text{m}$   $\text{InAlAs}/\text{InGaAs}$  high electron mobility transistors on GaAs," *IEEE Electron Device Lett.*, vol. 17, pp. 228-230, 1996.
- [3] S. Bollaert, Y. Cordier, V. Hoel, M. Zaknoute, H. Happy, S. Lepilliet, and A. Cappy, "Metamorphic  $\text{In}_{0.4}\text{Al}_{0.6}\text{As}/\text{In}_{0.4}\text{Ga}_{0.6}\text{As}$  HEMT's on GaAs substrate," *IEEE Electron Device Lett.*, vol. 20, pp. 123-125, 1999.
- [4] P. F. Marsh, S. L. G. Chu, S. M. Lardizabal, R. E. Leoni, III, S. Kang, R. Wohler, A. M. Bowlby, W. E. Hoke, R. A. McTaggart, C. S. Whelan, P. J. Lemonias, P. M. McIntosh, and T. E. Kazior, "Low noise metamorphic HEMT devices and amplifiers on GaAs substrates," in *1999 Microwave Theory and Techniques Symp.*, vol. 1, pp. 105-108.
- [5] P. F. Marsh, S. Kang, R. Wohler, P. M. McIntosh, W. E. Hoke, R. A. McTaggart, S. M. Lardizabal, R. E. Leoni, III, C. S. Whelan, P. J. Lemonias, and T. E. Kazior, "Millimeter-wave low noise metamorphic HEMT amplifiers and devices on GaAs substrates," in *1999 GaAs Integrated Circuit Symp.*, pp. 105-108.
- [6] M. Zaknoute, B. Bonte, C. Gaquiere, Y. Cordier, Y. Druelle, D. Theron, and Y. Crosnier, "InAlAs/InGaAs metamorphic HEMT with high current density and high breakdown voltage," *IEEE Electron Device Lett.*, vol. 19, pp. 345-347, 1998.
- [7] W. Contrata and N. Iwata, "Double-doped  $\text{In}_{0.35}\text{Al}_{0.65}\text{As}/\text{In}_{0.35}\text{Ga}_{0.65}\text{As}$  power heterojunction metamorphic on GaAs substrate with 1 W output power," *IEEE Electron Device Lett.*, vol. 20, pp. 369-371, July 1999.

- [8] C. S. Whelan, W. E. Hoke, R. A. McTaggart, P. S. Lyman, P. F. Marsh, S. J. Lichwala, and T. E. Kazior, "High power and gain at 35 GHz utilizing an  $\text{InAlGaAs/In}_{0.32}\text{Ga}_{0.68}\text{As}$  metamorphic HEMT," in *1999 GaAs Integrated Circuit Symp.*, pp. 1187-1190.
- [9] C. S. Whelan, W. E. Hoke, R. A. McTaggart, P. S. Lyman, P. F. Marsh, R. E. Leoni, III, S. J. Lichwala, and T. E. Kazior, "High breakdown voltage  $\text{InAlGaAs/In}_{0.32}\text{Ga}_{0.68}\text{As}$  metamorphic HEMT for microwave and millimeter-wave power applications," in *1999 Microwave Theory and Techniques Symp.*, vol. 3, pp. 1187-1190.
- [10] W. E. Hoke, P. J. Lemonias, J. J. Mosca, P. S. Lyman, A. Torabi, P. F. Marsh, R. A. McTaggart, S. M. Lardizabal, and K. Hetzler, "MBE growth and device performance of metamorphic high electron mobility structures fabricated on GaAs substrates," *J. Vac. Sci. Technol. B, Microelectron. Process Phenom.*, vol. 17, no. 3, pp. 1131-1135, 1999.
- [11] J. A. del Alamo, M. H. Somerville, and R. R. Blanchard, "Millimeter-wave power InP HEMTs: Challenges and prospects," in *European GaAs and Related III-V Compounds Application Symp.*, 1998, pp. 187-192.
- [12] N. A. Kozlov, V. F. Sinkevitch, and V. A. Vashchenko, "Isothermal current instability and local breakdown in GaAs FET," *Electron. Lett.*, vol. 28, no. 13, pp. 1265-1267, 1992.